Applied Geography 76 (2016) 37–48

Contents lists available at ScienceDirect

Applied Geography

journal homepage: www.elsevier.com/locate/apgeog

Coastal erosion and loss of wetlands in the middle Río de la Plata estuary (Argentina)

Francisco Cellone [a, *], Eleonora Carol [a], Luigi Tosi [b]

[a] Centro de Investigaciones Geológicas (CIG), Consejo Nacional de Investigaciones Científicas y Técnicas (CONICET-UNLP), Diagonal 113 N°275, B1904DPK, La Plata, Argentina

[b] Istituto di Scienze Marine, Consiglio Nazionale delle Ricerche, Arsenale Tesa 104, Castello 2737/F, 30122 Venezia, Italy

A R T I C L E I N F O

Article history:
Received 3 March 2016
Received in revised form
6 September 2016
Accepted 11 September 2016

Keywords:
Erosion
Coastal wetlands
Rates of shoreline change
DSAS

A B S T R A C T

Many worldwide coastal wetlands are facing erosion, severely putting at risk their noteworthy ecological functions. The Punta Indio coast, which bounds the Argentinean side of the middle Rio de la Plata Estuary, is experiencing noticeable shoreline retreat, as clearly shown by the occurrence of erosive features and wetland loss. The first step in understanding the causes of the coastal erosion is estimating the long-term historic evolution of the coastal changes. In order to overcome the unavailability of historical topographic data, we have used remotely sensed imagery (aerial photos and satellite images) to retrieve the multiple shoreline positions over the period 1943–2013. The rates-of-change and net shoreline movements have been computed by a statistical approach based on the Digital Shoreline Analysis System. Results point out that severe shoreline retreats (up to −7.4 m/yr) affect wide wetland sectors, especially where the natural intertidal vegetation is absent. In these areas, the native vegetation has been cut in the last century, and human activities such as tourism and settlements building experienced a strong development over the last decade. The simulated evolution of the coastline changes for the next 50 years shows that shoreline retreatments will take place very fast, about 4 m/yr. A general warning concerning possible consequences of severe degradation of the wetlands is given, while a remediation strategy, in conjunction with a coastal protection plan, are discussed.

1. Introduction

Many coasts of the world are suffering from severe erosion due to global and regional changes related to natural processes –sea-level rise, land subsidence, loss of sediment supply– and anthropogenic pressure –construction of coastal infrastructures and defenses, urbanization and other anthropogenic activities– (Ford, 2013; Mimura, 1999; Morris, Sundareshwar, Nietch, Kjerfve, & Cahoon, 2002; Nicholls et al., 2007; Zhang, Douglas, & Leatherman, 2004). Consequently, the hydrogeological hazard in the coastlands is increasing, as the natural protection provided by the beaches is vanishing.

The main role of coastal wetlands is their function as ecosystem-based coastal defenses; as such, they provide many important ecological and physical services, like the protection and mitigation of flood and surge events, pollution filtering, groundwater recharge, habitat for fish and wildlife (Odum, 1978, pp. 1–25). The most important natural function in stabilizing shorelines is played by wetland vegetation, which favors the sedimentation processes and reduces coastal erosion driven by storm surges (Anderson & Smith, 2014; Perillo, Wolanski, Cahoon, & Brinson, 2009; Feagin et al., 2011). However, coastal wetlands are fragile ecosystems, and shoreline erosion, as well as relative sea level rise, severe storm events, hydraulic reclamation, nutrient inputs and pollution, lead to their irreversible loss and degradation (Bird, Chua, Fifield, Teh, & Lai, 2004; Brinson & Malvárez, 2002; Kaiser, 2009; Michener, Blood, Bildstein, Brinson, & Gardner, 1997; Zedler & Kercher, 2005). Therefore, considering the valuable ecosystem services provided by coastal wetlands and their importance in driving local economies, e.g., fishing and tourism (Adamus et al., 1991, p. 297; Barbier, Acreman, & Knowler, 1997, pp. 1–27; Le Page, 2011, pp. 3–25), shoreline erosion and other causes of wetland degradation should be promptly monitored and studied.

Recently, the paradigm that wetlands provide shoreline protection was called into question (Feagin et al., 2011). In order to

* Corresponding author.
E-mail addresses: fcellone@fcnym.unlp.edu.ar (F. Cellone), eleocarol@fcnym.unlp.edu.ar (E. Carol), luigi.tosi@ismar.cnr.it (L. Tosi).

http://dx.doi.org/10.1016/j.apgeog.2016.09.014
0143-6228/

support the paradigm, Gedan, Kirwan, Wolanski, Barbier, and Silliman (2011) conducted a literature review and a small meta-analysis of wave attenuation data, finding that, in many instances, wetland plants reduce erosion, storm surge, and even small tsunami wave impacts. The Authors conclude that despite that the shoreline protection paradigm still stands, some gaps remain in the knowledge of the mechanistic and context dependent aspects of shoreline protection.

In Argentina, many coastland sectors are characterized by the presence of wetlands and most of them are included in protected areas, i.e. natural reserves sites of the world *heritage* network of the RAMSAR (Isacch, Escapa, Fanjul, & Iribarne, 2010). Despite these valuable ecosystems are protected, they undergo high ecological and physical pressures due to anthropogenic activity (e.g., Bértola, Cortizo, & Isla, 2009; Carol, Braga, Kruse, & Tosi, 2014; Codignotto, 2009; Isla, Cortizo, & Turno Arellano, 2011) and climate changes (e.g., Codignotto et al., 2011), which have led to significant coastal erosion (e.g., Pousa et al., 2007).

The Punta Indio District is located in the east margin of the middle estuary of the Río de la Plata, on the northeastern sector of Buenos Aires Province (Fig. 1). It is characterized by a humid and swampy region that comprises pampas grasslands and coastal wetlands, which are part of the biosphere reserves of the Buenos Aires province, recognized under the UNESCO's Man and the Biosphere Programme (MAB) (www.unesco.org/mab/). The importance of this area lays on its biodiversity. Within a limited area there are a large number of plant communities: *Vigna Luteola, Zizaniopsis bonariensis* (Espadaña), *Echinochloa helodes*, sedges, *Scirpus americanus* (totora), *Erythrina crista-galli* forest (Cagnoni, Faggi, & Ribichich, 1996; Vervoorst, 1967).

Punta Indio is a little town in the homonymous district, partly located in the wetland. Its socioeconomic development depends on the tourist activities carried out in the coastal zone where a serious shoreline retreat has been recently observed (Codignotto et al., 2011).

Due to the lack of previous studies and in-situ measurements, it is not fully understood when did coastal erosion begin and which is the main cause driving the shoreline retreat.

In order to overcome the lack of data, remote sensing archive images could provide an effective tool for the assessment of coastal changes (Kuenzer, van Beijma, Gessner, & Dech, 2014). Remotely sensed images are extensively used to calculate retreatment and progradation rates of shorelines by comparing multi-temporal images. However, the detection of the coastline position is affected by uncertainties, especially those related to the unknown time and meteo-climate conditions at the time of the image acquisitions, and to the proxy shoreline chosen by the operator. Many studies on the shoreline changes have utilized a uniform vertical level as a proxy shoreline, such as low or high water marks (Anders & Byrnes, 1991; Romine et al., 2009, 2013, pp. 149–57). Others, especially in micro-tidal environments, directly defined the shoreline position as the water line at the time of the photograph, taking into account the necessary corrections and uncertainties related to this value (Aiello, Canora, Pasquariello, & Spilotro, 2013). Moreover, errors related to digitizing and processing affect the detection of the shoreline position. Several studies have considered the errors and uncertainties related to mapping techniques, digitizing of the shoreline and imagery acquisition and processing. Considering these errors and uncertainties, it is important to produce reliable and statistically significant results (Anders & Byrnes, 1991; Crowell and Latherman, 1991; Moore, 2000; Morton, Miller, & Moore, 2004; Thieler & Danforth, 1994). When shoreline change is large, the error in shoreline positioning is relatively small; therefore, the erosion rates are reliable. Conversely, when shoreline change is smaller, the erosion rates become less reliable (Crowell, Leatherman, & Buckley, 1993).

This study is aimed at understanding past and expected morphological evolution of the Punta Indio littoral and factors responsible for shoreline erosion that are leading to significant wetlands loss.

We detect coastal changes using aerial photographs and satellite images acquired in the 1943–2013 period. Starting from the multiple shoreline positions, rates-of-change are computed and analyzed by a statistical approach based on spatial explicit methodology. Focusing on the sectors where coastal morphology resulted more dynamic, we discuss the cause-effect process, i.e. the relationship between past and expected long- and short-term shoreline changes, coastal erosion, loss of wetlands and development of built-up areas and coastal facilities for touristic needs. Concluding, a remediation plan is proposed.

2. Study area

This study focuses on the Punta Indio littoral, which is located at the right side of the Río de la Plata estuary, northeast sector of Buenos Aires Province, Argentina (Fig. 1).

The littoral of Punta Indio is formed by the Holocene depositional sequence, consisting of ancient tidal flats, a beach ridge plain, and recent marsh deposits (Cavallotto, Violante, & Parker, 2004; Fucks, Schnack, & Aguirre, 2010; Violante & Parker, 2004). The ancient tidal flat sector is represented by silt to clay sediments on surface, becoming sandier in depth; the beach ridge plain is represented by parallel systems composed of sandy and shelly deposits with finer textures between them. The present marshland is a narrow fringe parallel to the coast and it is composed of clay sediments. It constitutes an intertidal wetland where the hydrological and sedimentological processes are mainly regulated by tide action. Pleistocene loess-like deposits are exposed in the mainland while in the littoral they lay beneath the Holocene sequence. The geomorphological setting of the Holocene coastal plain is characterized by flat morphologies gently sloping toward the estuary, where ancient sandy beach ridges occur (Fig. 1). From the hydrogeological point of view, the ancient beach ridges allow the rainwater storage in shallow lenses, the only source of fresh groundwater, as the regional shallow aquifer is saline. The use of groundwater is generally limited because the risk of saltwater upcoming.

The Río de la Plata plays the main role in the sedimentary processes in the area under study. It discharges an average of about 22,000 m^3/s (Jaime, Menéndez, Uriburu Quirno, & Torchio, 2002), principally controlled by its two main tributaries, the Uruguay and the Paraná rivers, which are also the major sources of sediments, while the contribution of small creeks is negligible. The study area coincides with the maximum turbidity zone of the estuary, reaching sediment concentrations ranging from approximately 150 mg/L to 250 mg/L (Bazán & Janiot, 1991, pp. 65–91). The Río de la Plata estuary has a mixed semi-diurnal micro tidal regime characterized by a mean range of 0.71 m (Balay, 1961, p. 153). Tide flow direction alternates at intervals of 5–7 h and acts subsequently in the same and in the opposite direction to the river tributaries discharge. In some parts of the estuary this phenomenon pauses the flow and facilitates the decanting of transported sediments (Balay, 1961, p. 153).

However, because of the shallowness and increasing width of the Río de la Plata estuary, water level variations are strongly influenced by heavy SE-SSE winds, which can occasionally reach 75–88 km/h (D'Onofrio, Fiore, & Pousa, 2008). During storm surge events, locally known as “sudestadas” (southeasterlies), the water level of the estuary can raise more than 3 m, encroaching inland for several kilometers and producing a severe impact on the coast.

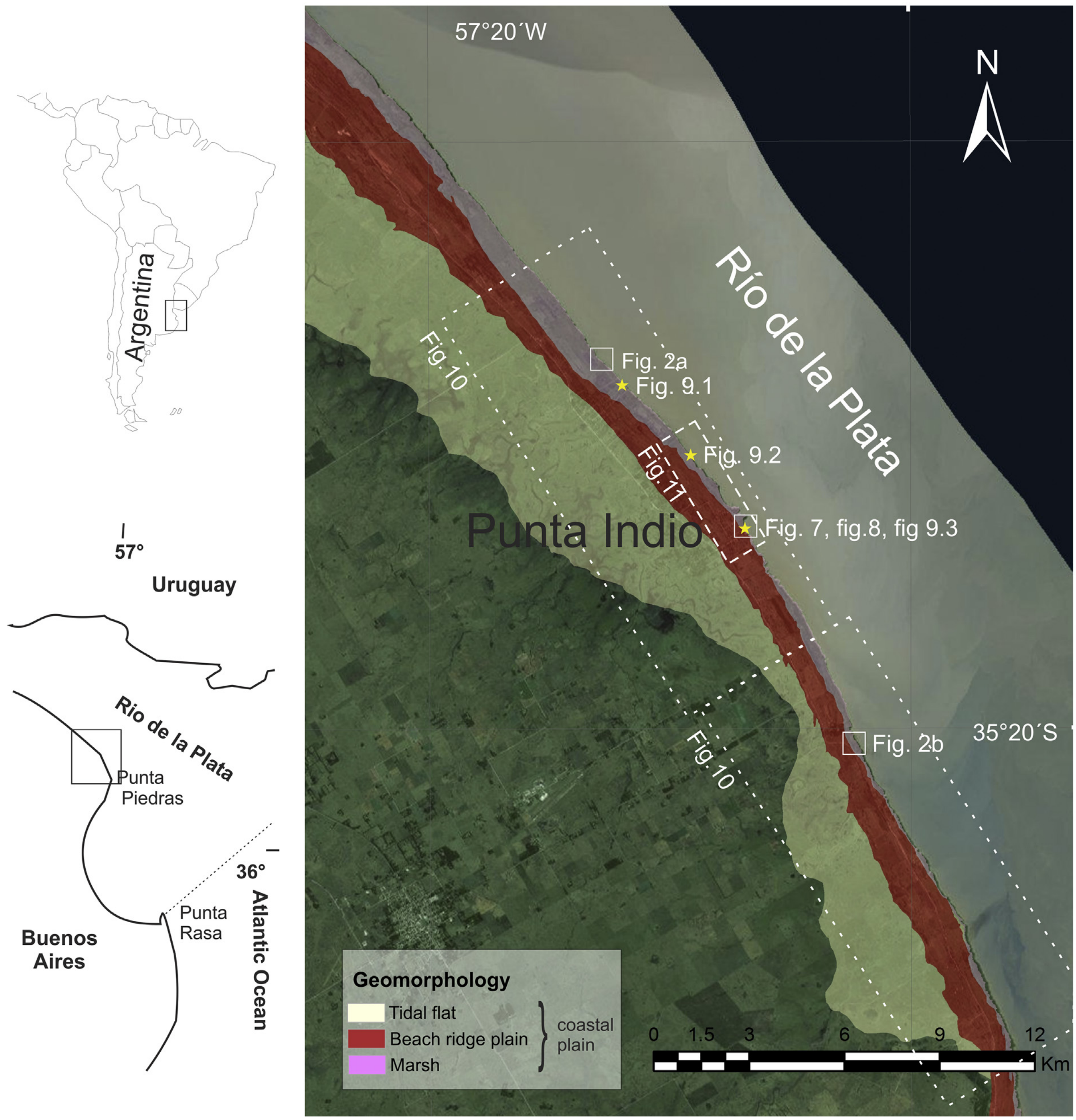

Fig. 1. Satellite image of the study area (from Bing imagery) showing the main geomorphological units of the Río de la Plata coastal plain at Punta Indio.

In addition, long-term coastal dynamics can be influenced by the relative sea level rise (RSLR), which can be reasonably assumed between 0.15 and 0.30 cm/yr, which are values calculated by Tosi et al. (2013) for the Samborombón Bay and Buenos Aires, respectively.

3. Materials and methods

Aerial photographs acquired in 1943, 1964, 1968, 1973 and 1987 and satellite images in 2003, 2010 and 2013 were used for this study. The 1943 and 1973 photos are from the Base Aeronaval de Punta Indio and the 1964 ones, were provided by the Instituto Nacional de Tecnología Agropecuaria (INTA). The 1968 and 1987 photos are from the Dirección de Geodesia de la Provincia de Buenos Aires. All available aerial photos are at 1:20000 scale. The 2003, 2010 and 2013 high resolution satellite imagery (e.g., GeoEye-1, Ikonos and WorldView-2) were downloaded at different scales from Google Earth archive (Digital Globe imagery).

The aerial photographs and satellite images were geo-referenced in the WGS84/TMARG6 projection system using a variable number of control points. Each aerial photograph and satellite image was geo-referenced separately, and control points (e.g., coastal infrastructure, roads, house, bridges) were selected by comparing each image with digital cartography from the Argentinian "Instituto Geográfico Nacional". The digital cartography consists in vector information residing in a constantly updated GIS platform, and includes railroad network, road network, infrastructure and other geographical features. Additional geo-referenced points were obtained from topographic surveys performed in years 1932, 1939, 1941, 1964 and 1971.

The multi-temporal coastline positions were detected using the edge of vegetation as a proxy to map shoreline positions (Ford,

Table 1
Characteristics of the remote sensed imagery and geo-referencing errors.

Image	Pixel size (m)	Geo-ref. min (m)	Geo-ref. max (m)	Transformation	Total shoreline error (m)
1943 B/W aerial	3	5.5	9.4	2nd order polynomial	9.8
1964 B/W aerial	0.5	0.0	0.0	Spline	1.2
1968 B/W aerial	0.5	1.5	3.6	1st order polynomial	3.8
1973 B/W aerial	0.5	1.9	1.9	2nd order polynomial	2.2
1987 B/W aerial	0.5	2.1	2.1	2nd order polynomial	2.3
2003 Digital Globe	0.8	0.3	1.9	2nd order polynomial	2.3
2010 Digital Globe	0.5	1.5	2.2	2nd order polynomial	2.4
2013 Digital Globe	0.5	0.2	2.7	2nd order polynomial	2.9

2013). This approach overcomes any uncertainty related to the comparison of shoreline positions detected at different tide conditions.

The multi-temporal analysis of shoreline changes was performed using the Digital Shoreline Analysis System (DSAS 4.3) (Thieler, Himmelstoss, Zichichi, & Ergul, 2009). DSAS allows computing rate-of-change statistics from multiple historic shoreline positions residing in a GIS. It automatically casts a number of regularly spaced transects perpendicularly to a user-created baseline, and uses the intersections between them and the digitalized shorelines to perform statistics. In addition, it allows to set a threshold to the minimum number of shorelines used in the calculus and the values of each shoreline uncertainties.

In this work, DSAS has been used to calculate the Weighed Linear Regression (WLR) and the Net Shoreline Movement (NSM), which represent a weighted value of the shoreline change rate and the total distance between the oldest and youngest shorelines, respectively.

The weight (w) is defined as a function of the variance in the uncertainty of the measurement (e) (Genz, Fletcher, Dunn, Frazer, & Rooney, 2007):

$$w = 1\Big/\left(e^2\right)$$

where e is the shoreline uncertainty value.

DSAS requires the following inputs: the digitized shoreline time-series, the mapping uncertainty for each shoreline, the user-created baseline and user-selected transect spacing.

The mapping uncertainty is used by DSAS for calculating the WLR for each shoreline. Different methods have been proposed by various authors to assess the shoreline mapping uncertainties. Morton et al. (2004) used the root sum of digitizing, map survey, photogrammetric and GPS errors. Romine et al. (2013, pp. 149–57) identified as sources of errors the original field survey, the image rectification and digitalization, the pixel size, the occurrence of waves and the tidal fluctuation, and calculated the total uncertainty by the root sum of all these errors.

In this study, the non-availability of the acquisition times of the remotely sensed images prevents against the evaluation of the tidal fluctuation errors. Therefore, we adopted a method that uses the root sum of pixel size error, rectification error and digitizing error, as proposed by Ford (2011, 2013). This method does not require tide measures to evaluate tidal fluctuation errors and is simpler than those proposed by Morton et al. (2004) and Romine et al. (2013, pp. 149–57). The assumption of not considering tidal fluctuation errors is supported by the fact that the whole image data set (excluding the 2013 set) shows the aerial exposure of the abrasion platform next to the coastline, i.e. the estuary bottom. Hence, this assured that images were acquired during quite similar low tide conditions. Seasonal errors, such as changes in shoreline shape due to waves and storm surges, were not considered because there was no

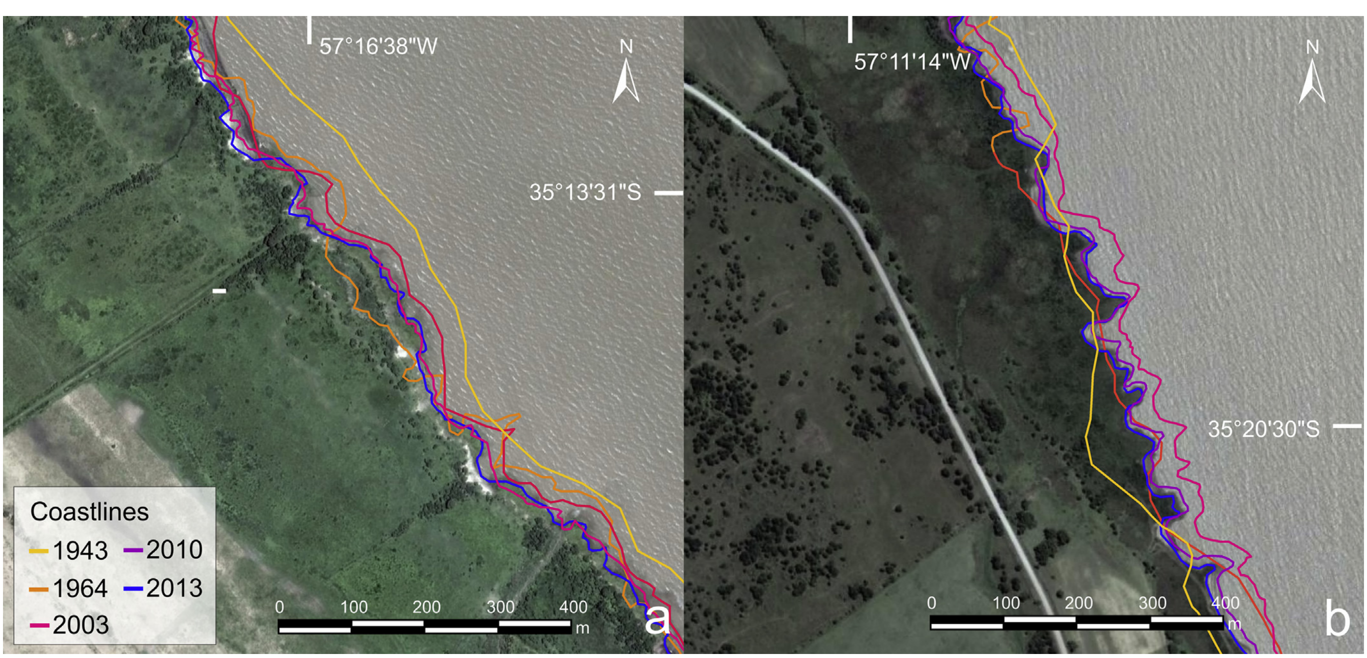

Fig. 2. Examples of coastline changes local variability over the 1943–2013 period. The positions of a, b are shown in Fig. 1.

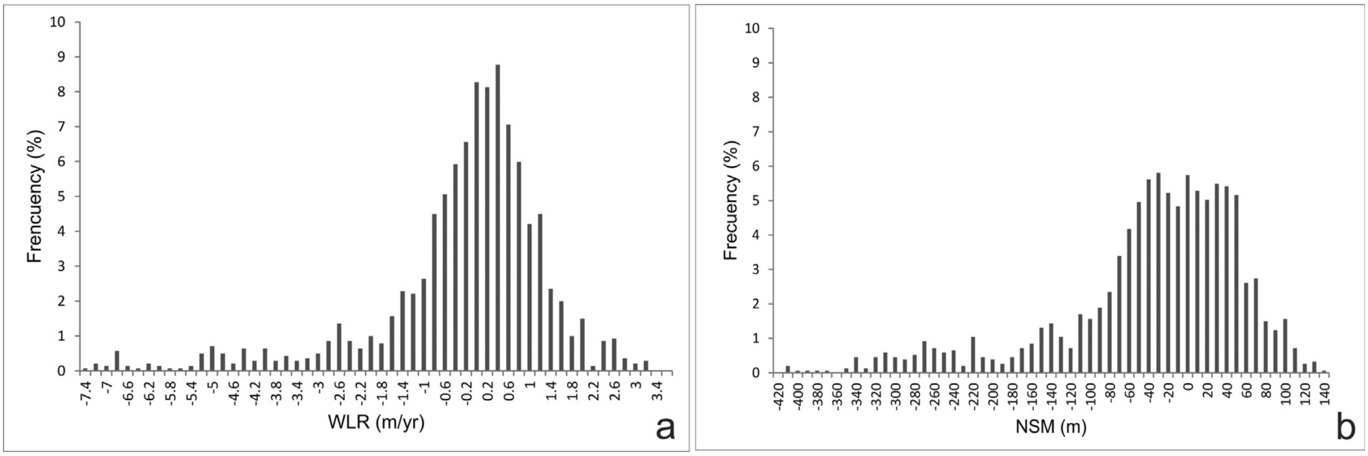

Fig. 3. Frequency distributions of WLR (a) and NSM (b) for the whole coast.

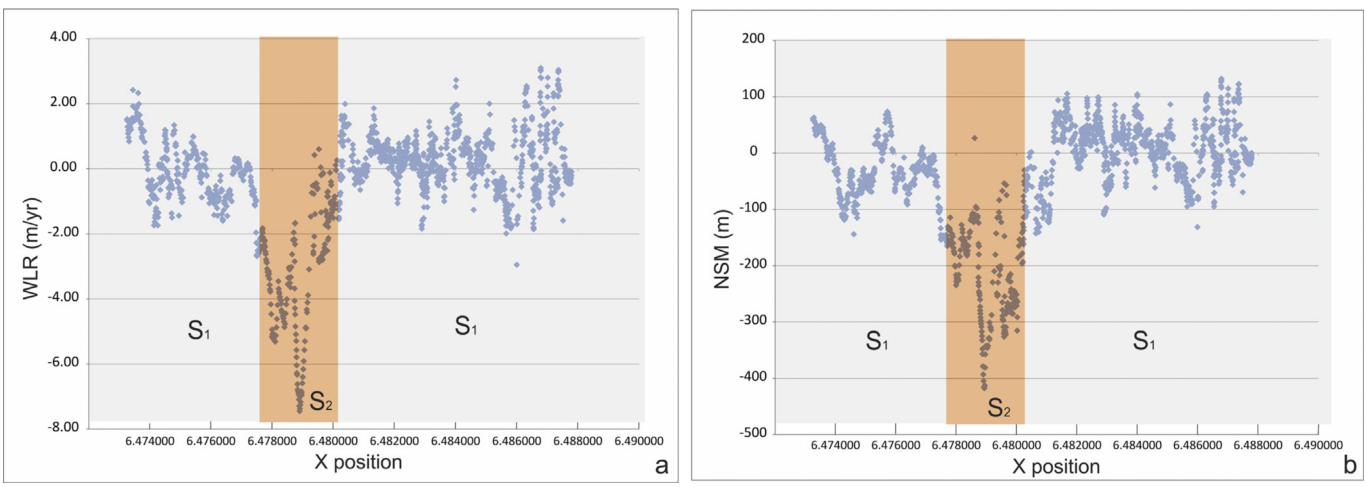

Fig. 4. Spatial distribution of the WLR and NSM values along the whole coast.

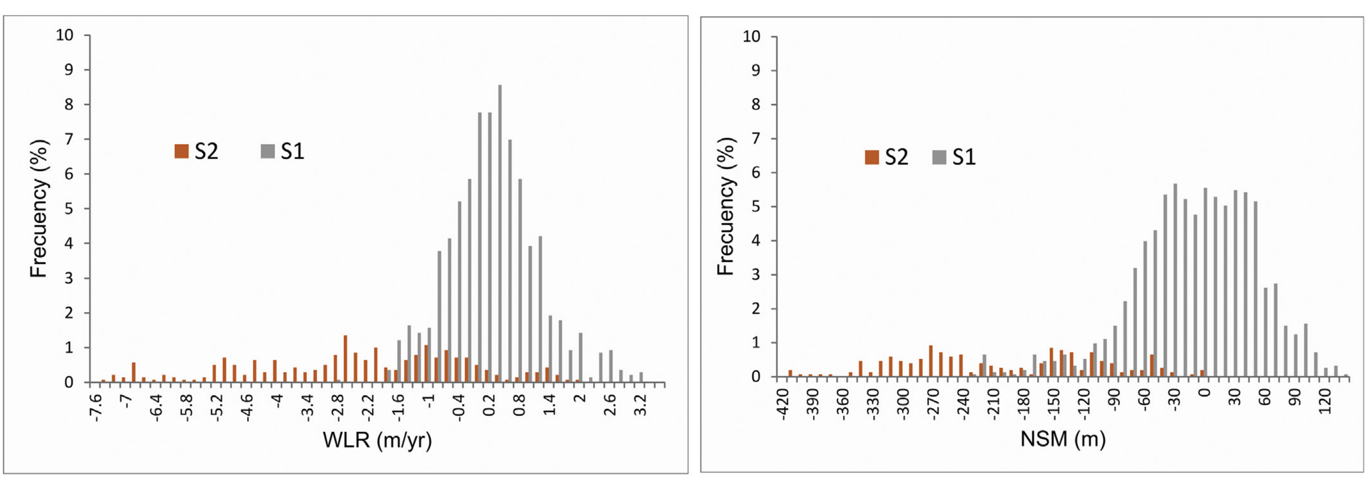

Fig. 5. Frequency distribution of the WLR (a) and NSM (b) values.

evidence of their occurrence, and their effect is limited in a long-term analysis. The digitizing error was taken from the maximum digitizing error estimated in previous studies adopting a value of 1 (Anders & Byrnes, 1991; Crowell and Latherman, 1991; Moore, 2000; Morton et al., 2004; Thieler & Danforth, 1994). The rectification error was taken as the maximum RMS error calculated for each time period when the images were geo-referenced. First order polynomial, second order polynomial and spline transformations

Table 2
Rate-of-change statistics of the multiple historic shoreline positions for the period 1943–2013 obtained by DSAS.

Sector S1	Sector S2	Whole coast	
Average WLR (m/yr)	0.1	−3.6	−0.4
WLR Standard deviation	0.9	1.8	1.7
Maximum WLR (m/yr)	3.1	0.6	3.1
Minimum WLR (m/yr)	−2.9	−7.4	−7.4
Average NSM (m)	−13.9	−204.5	−41.4
NSM Standard deviation	66.8	83.7	95.5
Maximum NSM (m)	131.9	−53.8	131.9
Minimum NSM (m)	−315.4	−417.5	−417.5

were used. The transformations were selected based on the minimum values of RMS. Errors range between 0.0 and 9.4 m, and only the maximum geo-referencing error for each group of images was used to calculate the total uncertainty (Table 1). The total mapping uncertainty ranges between 1.1 and 9.8 m (Table 1).

On the base of the study area extent and the digitalized shoreline resolution, the 20 m spacing between transects resulted the less time-consuming option. A total number of 1402 transects was generated.

The baseline, which is an arbitrary line, manually drawn behind the inner shoreline, is used by DSAS as reference for casting transects that intersect the digitized shorelines considering an appropriate scale and the different orientation of the shoreline positions. The program records the position of the intersections between transects and each shoreline and uses them to calculate Net Shoreline Movenment and Weighted Linear Regression (WLR).

Considering that there are some gaps in the remote sensing data archive, and only the 1943 and 2013 imagery covers the entire area, a shoreline intersection threshold of 3, i.e. the minimum number of shorelines intersecting the casted transects, was adopted for the statistical analysis of WLR. Therefore, the calculation of WLR was possible only where 3 shorelines intersect each transect. The baseline is not considered in the intersection threshold. Because the occurrence of the intertidal vegetation along the coast plays an important role in coastal dynamics (Isacch et al., 2010), the *Vigna*

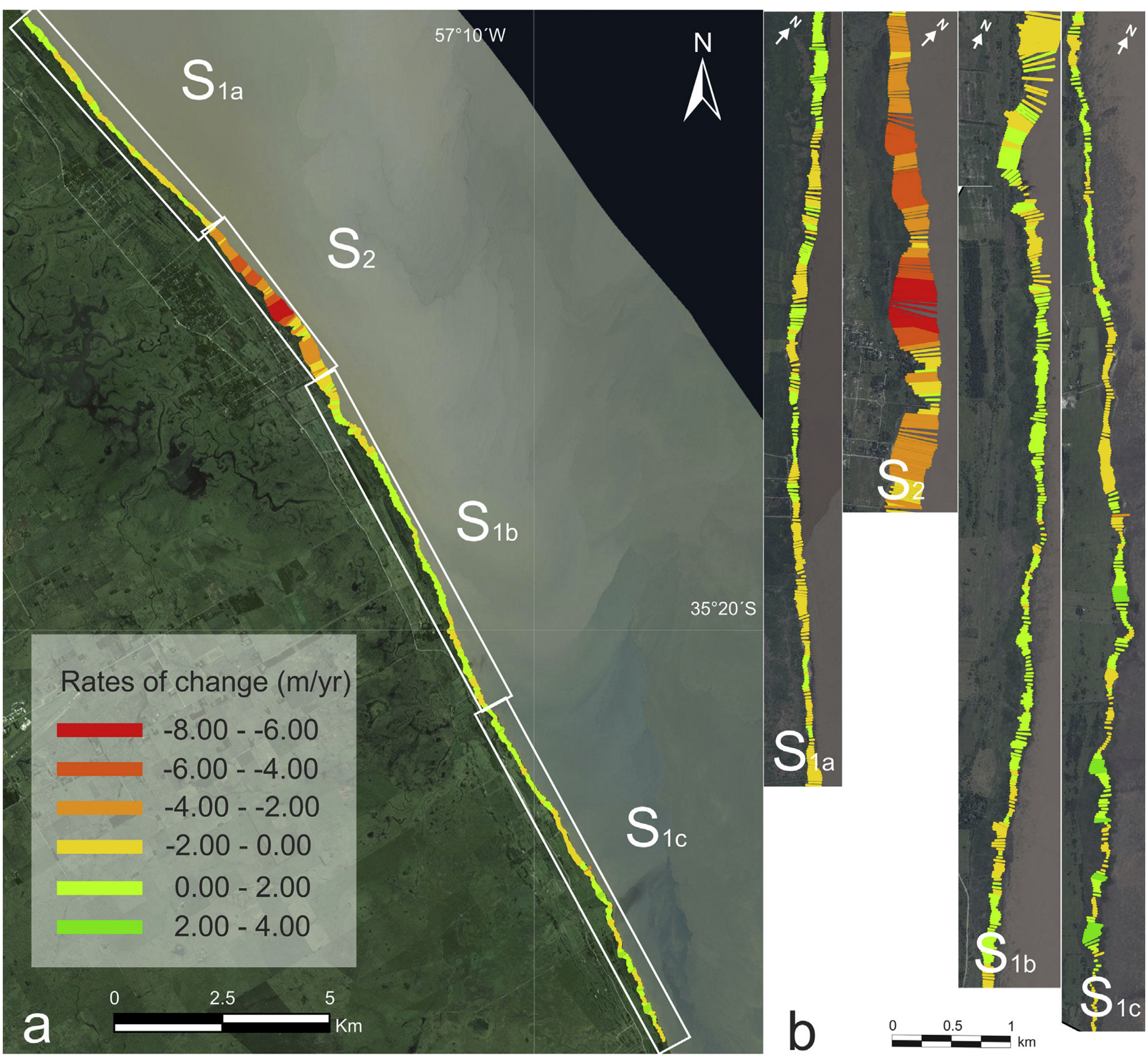

Fig. 6. a) Map of the 20-m spaced transects calculated by DSAS and classified on the base of WLR values. S1 and S2 sectors are divided in S1a, S1b, Sc to assure a better visualization of transects. b) Enlargements of the four S sectors. Satellite image background is from Bing imagery.

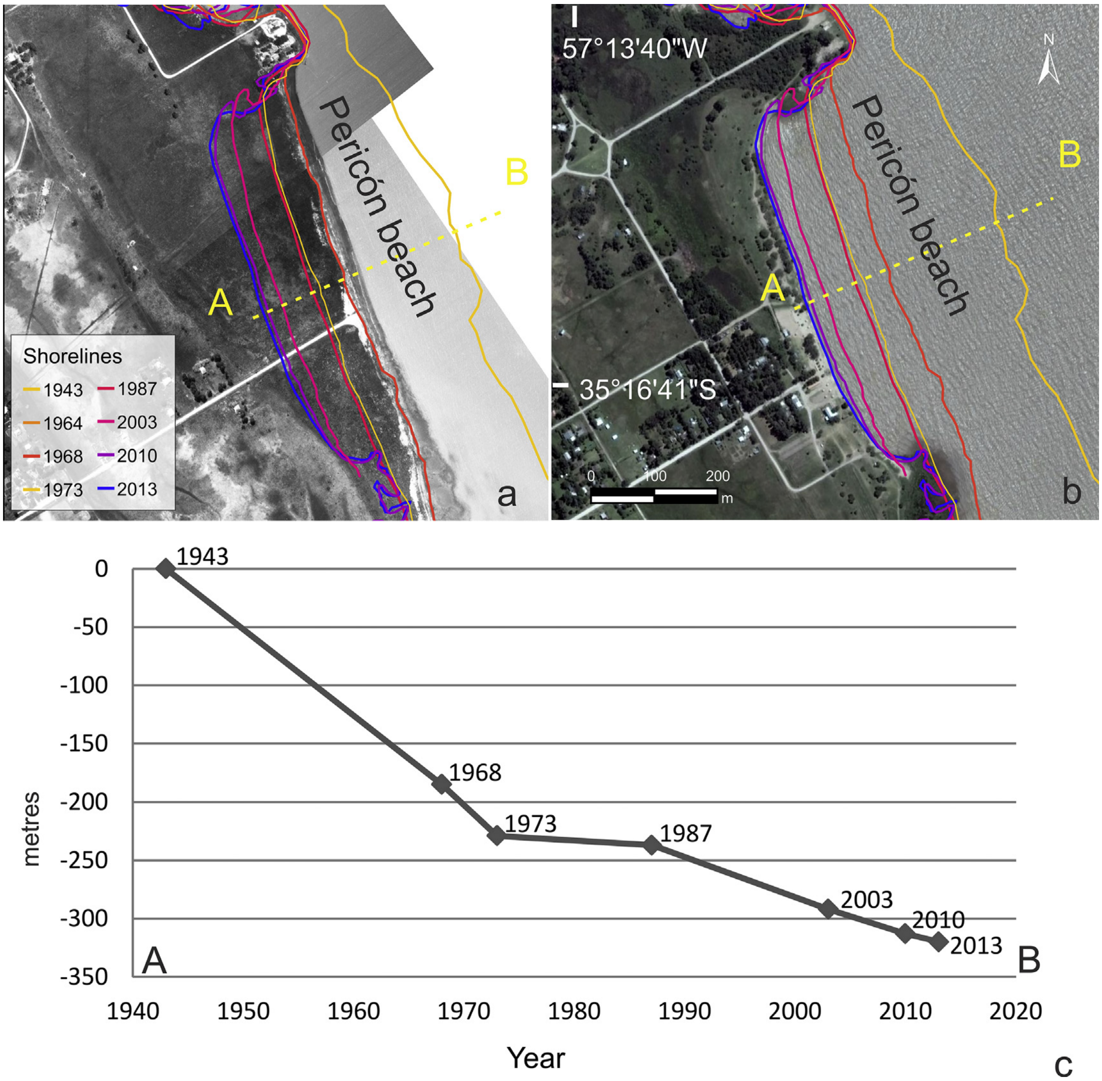

Fig. 7. Map of coastline change occurred in the 1943–2013 period at Pericón beach superposed to the 1968 aerial photograph (a) and the 2013 satellite images (b). c) reports the NSM values calculated along a single transect representing the zone more affected by shoreline retreatment. The positions of a and b are shown in Fig. 1.

luteola community (the native intertidal vegetation principally represented by *Scirpus americanus*) was mapped in order to compare vegetation and non-vegetation presence with the WLR values. The 2013 satellite image was selected for mapping the vegetation, because no field surveys were performed previously to assess the correspondence between the imagery patterns and the presence of the intertidal vegetation.

The last analysis was the assessment of the future evolution of the coastline for 10, 20 and 50 years from 2013. The predicted future shoreline positions were based on the linear extrapolation of the WLR values. To assure a better prediction of the coastal evolution, only transects exhibiting values of WR2 (r-squared) between 0.8 and 1 were used (Maiti & Bhattacharya, 2009). Finally, the expected coastline positions were manually drawn based on the lengths of the extrapolated transects.

4. Results

4.1. Net shoreline movement and Weighted Linear Regression analysis

The characterization of the coastal change occurred between 1943 and 2013 in the Punta Indio coast is particularly complex due to the high variability of the shoreline movements both at temporal and local scales (Fig. 2).

The result of the analysis of the multiple historic shoreline positions obtained by DSAS shows that the mean values of WLR and NSM are −0.4 m/yr and −41.4 m, respectively. Although these values suggest a general low retreat of the whole coastline, their high standard deviations, 1.7 m/yr for WLR and 95.5 m for NSM, imply a high heterogeneity of the coastline movements, probably at local sectors. In addition, the frequency distributions of these parameters are clearly asymmetric (Fig. 3) and span between 3.1 and −7.4 m/yr for the WLR and between 131.9 and −417.5 m for the NSM.

The analysis of spatial distribution of the WLR and NSM values along the whole coast was performed in order to point out sectors with similar coastal dynamics (Fig. 4). The result shows a significant alternation of negative and positive values of the shoreline movements at local scale in the Northern and Southern sectors. In addition, Fig. 4 points out that a noteworthy number of transects – characterized by WLR less than -2 m/yr and NSM less than −100 m– is placed next to the central sector. This suggests the necessity to analyze separately transects corresponding to different behaviors of the coastline movements. The spatial distribution of the WLR values allowed to distinguish two main groups of zones characterized by general values higher and lower than −2 m/yr, S1 and S2 sector, respectively.

Fig. 5 reports a remarkable difference in the frequency distribution of the WLR and NSM values for the sectors S1 and S2. A Gaussian distribution with zero mean characterizes transects falling in the S1 sectors, while a mainly negative and multimodal distribution is observed for those transects represented on the S2 sector.

In S1 sectors, WLR ranges between 2.9 and - 3.1 m/yr with a mean of 0.1 m/yr and a standard deviation of 0.9 m/yr. The NSM values span from −315.4 to 131.8 m, with an average of −13.9 m and a standard deviation of 66.8 (Table 2).

In sector S2, WLR is in the range −7.4–0.6 m/yr, averages −3.6 m/yr with a standard deviation of 1.8 m/yr. The values of the NSM are between −417.5 and −3.4, with average and standard deviation, of −204.5 m and 83.7, respectively (Table 2).

Fig. 6 reports the classification of the transects based on the WLR values computed by DSAS and the positions of S1 and S2 sectors. S1 sectors show alternating spatial pattern of positive and negative values of WLR, whereas the S2 sector is mainly characterized by higher negative values.

The Pericón beach, located in the Punta Indio town (sector S2), is a relevant example of a coastal sector affected by severe shoreline retreatment. The evolution of the shoreline position over the 1943–2013 period is shown in Fig. 7a and b. The total amount of coastal retreatment occurred over the whole period is 320 m, with WLR values ranging from −2.3 to −2.9 m/yr. Fig. 7c reports the relationship between NSM values and the corresponding year along a single transect (Fig. 7c).

The Pericón beach is characterized by coarse sands instead of fine sediments because artificial nourishment was done for touristic purposes. Fig. 8 reports two photographs of a sector of this beach taken during different tide conditions, in May 2014 and in March 2016, with tide levels of 1.2 m and 0.9 m, respectively. Although these photographs do not allow a direct comparison of the two coastline positions, they show evidences that an indisputable erosional process is in act and severely affects this beach. For instance, it is to note the presence of erosional scarp and the exposure of the roots of vegetation (*Salix*) at the edge of the wetland. In addition, the May 2014 photograph shows an alignment of remnant *Salix* not occurring in the image taken in March 2016 because they were removed by the erosion.

The erosive process of the Pericón beach began after the cutting of the natural vegetation (e.g., *Scirpus americanus*) and is still active because of its absence and the nourishments not properly done.

4.2. Wetland vegetation and coastal changes

The result of the analysis of the intertidal vegetation occurrence and shoreline changes, points out a significant correlation between shoreline retreat and loss in intertidal vegetation and, vice versa, between the presence of native vegetation and advancement or at least stability of the beach. Fig. 9 reports three examples highlighting the shoreline erosion and stability in different zones of the Punta Indio coast (1, 2 and 3). In areas with presence of healthy and well developed natural vegetation on the edge of the wetland, the shoreline changes are negligible (Zone 1). On the contrary, the sectors with sparse or even absent natural vegetation are characterized by relevant erosional features (Zones 2 and 3).

Fig. 10 shows a map of the distribution of natural intertidal

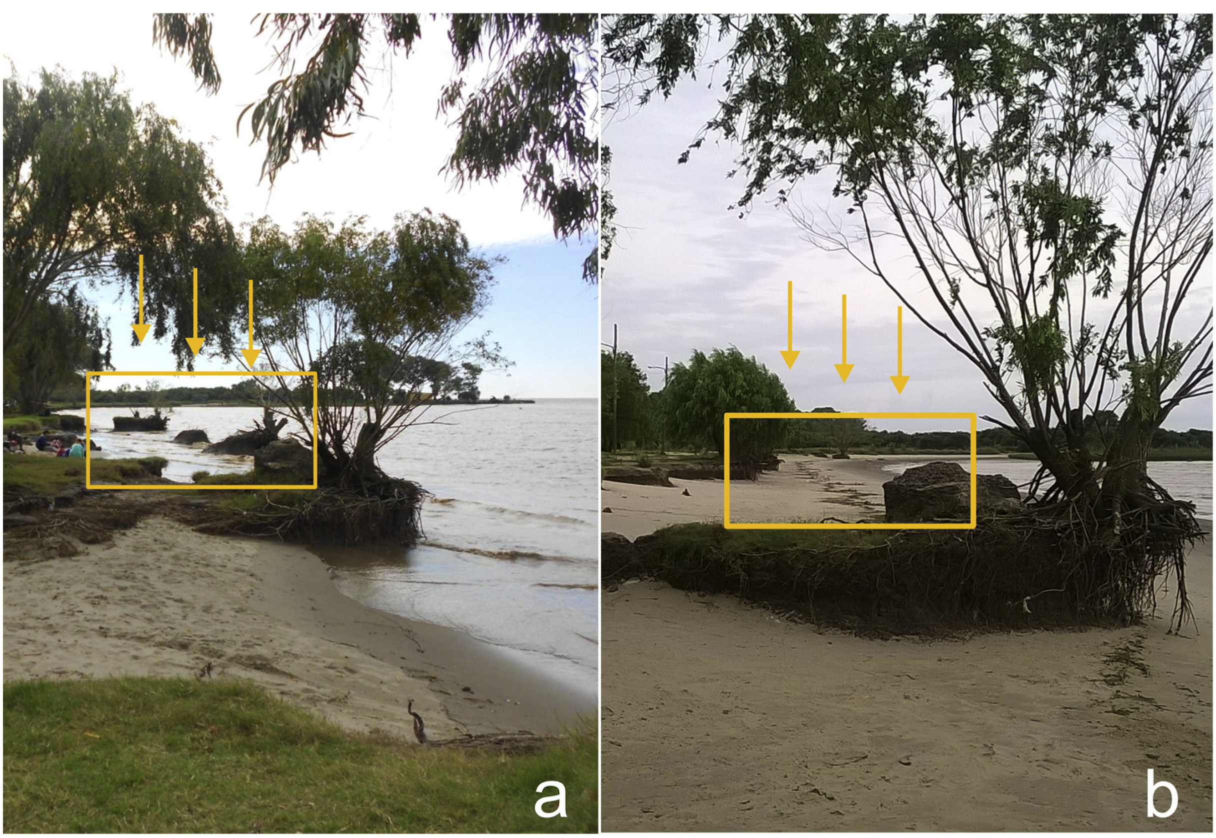

Fig. 8. Erosion of the Pericón beach: a) May 2014 (b) March 2016. The arrows show the alignment of remnant Salix roots that are present in May and not in November 2014. The positions of a, b are shown in Fig. 1.

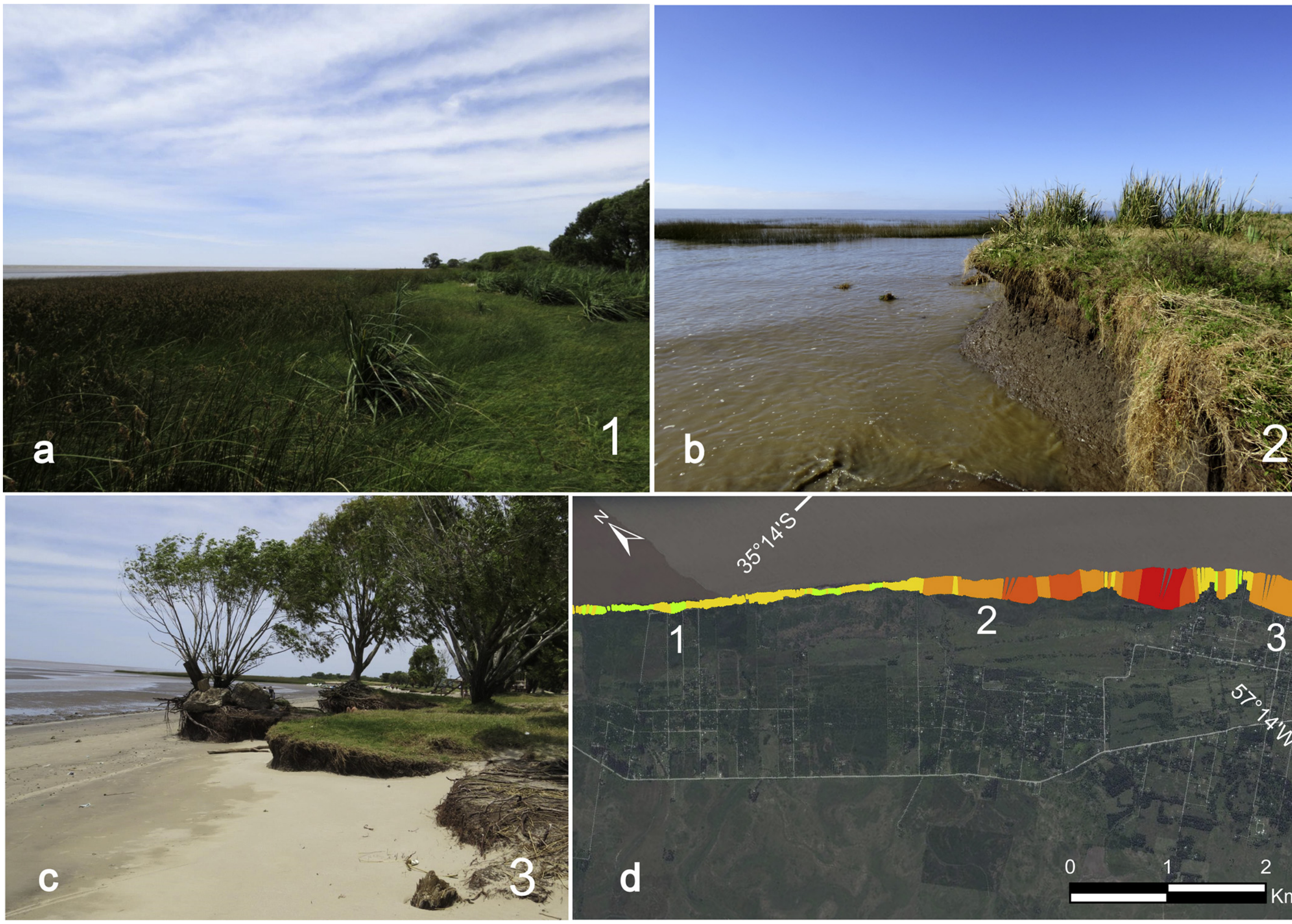

Fig. 9. Erosion and stability of shoreline in three zones of Punta Indio coast: a) presence of natural intertidal vegetation in a case of shore advancement (zone 1, Sarandi beach); b) and c) missing of natural vegetation and presence of erosional scarp (zones 2 and 3); d) detail of the WLR analysis for the Punta Indio coast. The positions of a, b, and c images are shown in Fig. 1.

vegetation occurring in 2013 along with the position of WLR transects characterized by positive values. Their comparison points to a clear correlation between positive WLR values and presence of natural intertidal vegetation. In this case, the mean shoreline change is 0.5 m/yr, with a standard deviation of 0.3 m/yr. Conversely, in the zones where the vegetation is absent the mean shoreline change is −1.2 m/yr, and the standard deviation is 1.9 m/yr. In the case of NSM the average values are −8.9 m and −78.0 m for vegetation and non-vegetation sectors, respectively. Therefore, the presence and absence of natural vegetation likely explain the asymmetry in the frequency distributions of WLR and NSM as previously shown in Fig. 3. Fig. 10c and d are detailed satellite images that show sectors of the coast where the natural intertidal vegetation is respectively present and absent.

4.3. Shoreline evolution

A detailed shoreline evolution has been provided for the sector S2 (see Fig. 6) where the whole imagery dataset is available. Past and recent shoreline positions have been retrieved by 7 images, i.e. 1943, 1968, 1973, 1987, 2003, 2010 and 2013, while the expected evolution of the shoreline position has been calculated for 2023, 2033 and 2063. Considering the extrapolation of the actual rates of shoreline change, noteworthy erosion in this zone of the study area is predicted with a mean shoreline change rate of −3.8 m/yr.

Forecast scenarios show that wide areas of the Punta Indio wetland are expected to disappear within 10–20 years (Fig. 11). In addition to the ecological degradation, coastal infrastructure will be severely affected in a relatively short-time. For example, in Pericón beach coastal retreatment is already jeopardizing the touristic facilities. At the turn of 2063, the erosion will extend more than 160 m to the inland sector. This coastal retreat will cause disappearence of almost the whole wetlands and the irreversibly vanishing of their ecosystem-based service. Urban settlements and infrastructures at that time will have been severely damaged, impacting the socioeconomic development of the Punta Indio region.

5. Discussion

This work shows that wide sectors of the wetlands forming the Punta Indio coast suffer from shoreline erosion. The higher erosional rates are linked to the absence of the natural wetland vegetation. Hence, the ability of wetlands to trap sediments coming from the Rio de La Plata Estuary, to reduce wave and storm surge impacts, as well as their capacity to regulate nutrient fluxes and provide habitat are significantly reduced or have even vanished.

Besides the fact that there are no records and information on the original extent of the intertidal wetland vegetation, its loss seems to be primarily caused by human activities. Where the vegetation

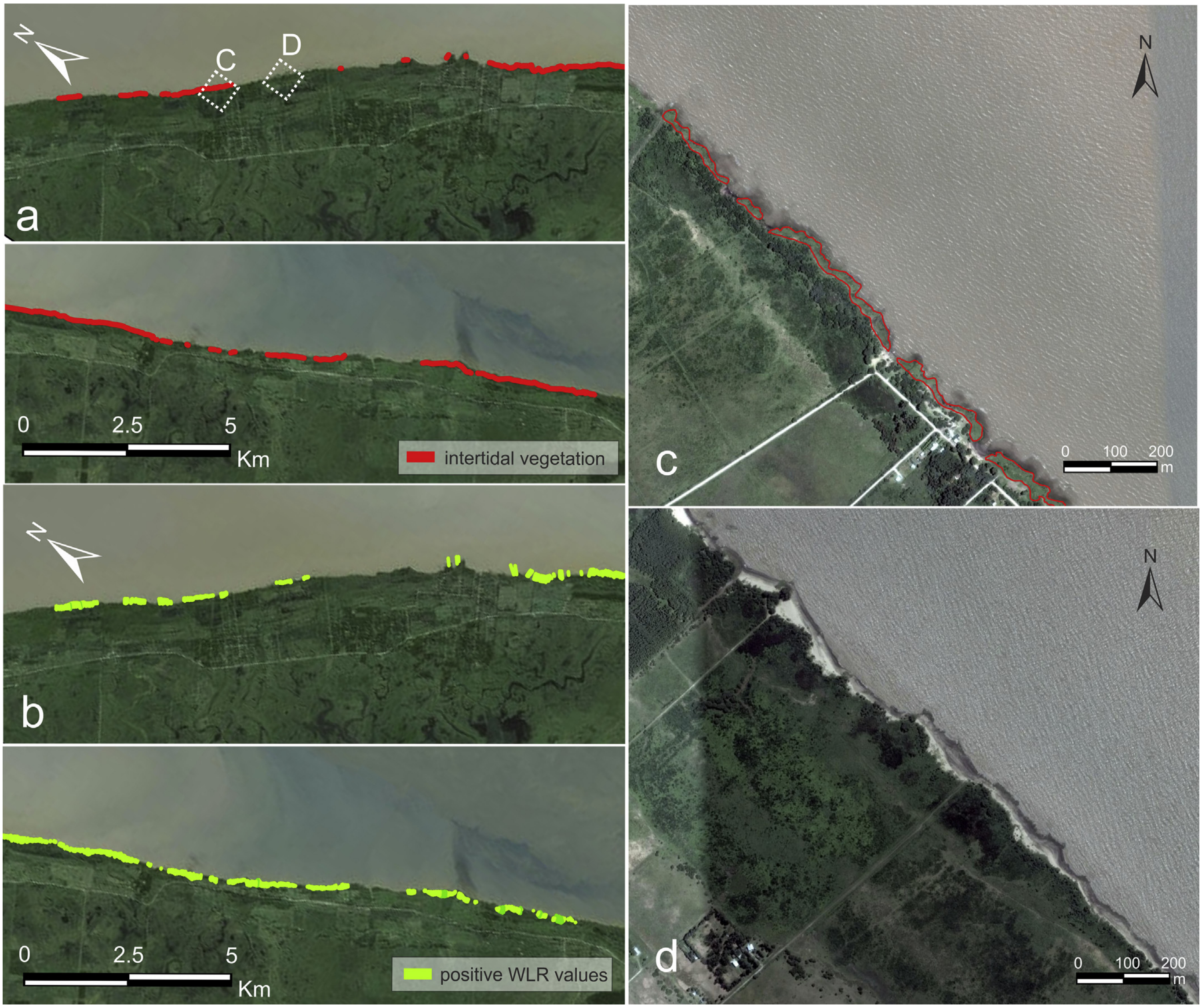

Fig. 10. Maps of the intertidal vegetation occurrence in 2013, distribution of the positive values of WLR and detailed images of the intertidal vegetation occurrence and absence. a) Intertidal vegetation occurrence along the whole coast. b) Transects exhibiting positive values of WLR. c) Sector of the coast, pointed in (a), where the intertidal vegetation is present. d) Sector of the coast, pointed in (a), where the intertidal vegetation is absent. The positions of a, b, c and d images are shown in Fig. 1.

has been cut, the erosion led to a continuous shoreline retreatment, subsequently inhibiting the natural restoration processes. Considering the increase in frequency of the storm surges pointed out by D'Onofrio et al., (2008) and the RSLR occurring at regional scale (Tosi et al., 2013), we reasonably believe that also these processes have contributed to the shoreline erosion and loss of wetlands. Regarding the coastal erosion driven by land subsidence induced by the groundwater exploitation, we can state that the urban development has not yet reached such extensions to significantly reduce the groundwater recharge provided by rainfalls, as shown in other coastal areas (e.g., Carretero, Braga, Kruse, & Tosi, 2014), and the increase of groundwater pumping to cope with the request of water supply during summer is limited by the risk of upcoming saline contamination of the freshwater reserves.

The simulated evolution of the coastline changes for the next 50 years shows that the degradation of the wetlands will take place very fast, in the order of −3.8 m/yr. However, this represents an optimistic scenario, because the simulation does not consider (i) the erosional effect due to the increasing frequency of the storm surges (D'Onofrio et al., 2008), (ii) the expected relative sea level rise (Tosi et al., 2013), and (iii) the increasing development of tourism activities.

Under these future prospects of negative evolution of wetlands, it would be imperative to implement a management plan for the sustainable development of the Punta Indio coastal area, including countermeasure strategies, as well as protection and mitigation interventions, at least to slow down the erosive processes. In contrast to the traditional structures for controlling the coastal erosion such as bulkheads, stone revetments and seawalls, there is a new paradigm: "living shorelines" (National Research Council, 2007). These systems consist on the simultaneous construction of artificial structures and restoration of natural vegetation, which give the same protection as traditional defense structures with the additional benefits of ecological restoration, environmental and biodiversity conservation (Gedan et al., 2011; Swann, 2008). Among the various methods, there are many restoration plans developed in

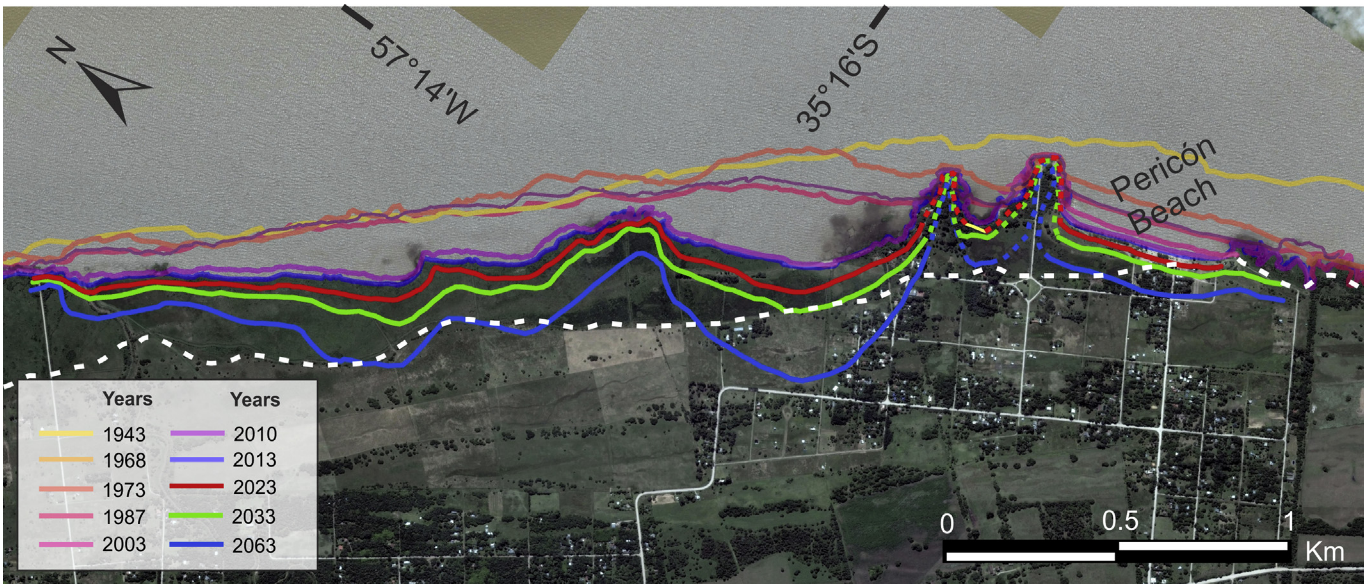

Fig. 11. Past and expected shoreline changes at Punta Indio. The white dotted line indicates the wetland boundary. The position of the image is shown in Fig. 1.

salt marshes, where the implementation of oyster domes, oyster reef, reef balls or oyster cultch (concrete structures that baffle waves and provide habitat for benthic ecosystem engineers) in conjunction with the restoration of the natural intertidal vegetation of *Spartina alterniflora*, has had good results (Gedan et al., 2011; Meyer, Townsend, & Thayer, 1997; Piazza, Banks, & La Peyre, 2005). These structures allow the restoration of the vegetation in places experiencing high shoreline change rates or being frequently exposed to storm surges. With similar results regarding sediment accretion and shoreline change rates reduction, Swann (2008) implemented coastal havens, highlighting their capability of self-maintenance and the possibility of their removal and relocation. Smaller scale restoration projects may be justified because even narrow wetlands can dampen waves as wave attenuation is non-linearly correlated with transverse distance (Gedan et al., 2011).

In the central sector of the study area, at Punta Indio, where the highest negative shoreline change rates have been measured and the natural intertidal vegetation is absent (Fig. 11), it would be recommendable to implement a restoration plan of the natural vegetation (*Vigna luteola* community), along with the construction of structures such as oyster cultch or oyster domes, that tend to reduce wave energy and storm surge effects on the coast.

6. Conclusions

This study is the first approach aimed to quantify the rates of shoreline change and the net shoreline movements of the Punta Indio shoreline.

Results of the analysis show the existence of a coast section characterized by severe shoreline erosion, whose average rate of −3.6 m/yr deviates from the normal behavior of the rest of the coast (−0.4 m/yr).

A significant relationship between the presence of the intertidal vegetation and the shoreline dynamic behaviors is also observed. Specifically, the highest negative shoreline movements were measured in the areas where the natural intertidal vegetation is absent and erosive features are clearly shown. This highlights that the triggering of the erosion process is due to the cutting of natural vegetation on the wetlands for developing human activities such as tourism and settlements.

The 10-, 20-, and 50-year shoreline evolution expected at Punta Indio points out a significant retreatment of the shoreline up to 3.8 m/yr, which would not only affect the sustainability of the wetlands but also the development and infrastructure in the town of Punta Indio. Furthermore, the socioeconomic development of the area, in conjunction with the mean sea level rise and the increasing frequency of storm surges, would aggravate the vulnerability of the coastal wetlands.

Regarding the future prospects of the Punta Indio littoral, the protection of the wetlands becomes essential, as well as the implementation of management plans designed to allow a sustainable development of the coastland. On the base of previous restoration plans leading to successful results in other areas with similar characteristics, we propose the implementation of solutions under the paradigm of living shorelines.

Coastal erosion is a problem that affects many coastal wetlands along the world. The lack of in situ measurements can be overcome by the use of remote sensing techniques, which have the advantage of providing long-term multi-acquisition image archives. While this work provides the first analysis of the shoreline changes of the Punta Indio coast, revealing the seriousness of the wetland loss, it also offers a methodology that can be used to investigate other coastal wetlands worldwide lacking in-situ measurements.

Acknowledgments:

The authors are very indebted to the Agencia Nacional de Promoción Científica y Tecnológica (National Agency for Scientific and Technological Promotion) and the Consejo Nacional de Investigaciones Científicas y Técnicas (National Council for Scientific and Technological Research) of Argentina for financially supporting this study by means of their grant, PICT 2013–2248. Further, the authors would like to thank the Base Aeronaval Punta Indio for their collaboration providing aerial photographs from the coast.

References

Adamus, P. R., Stockwell, L. T., Clairain, E. J., Jr., Morrow, M. E., Rozas, L. P., & Smith, R. D. (1991). Wetland evaluation technique (WET). In *Literature review and evaluation rationale* (Vol. 1). Vicksburg, MS, USA: Environmental Laboratory, US Army Engineer Waterways Experiment Station.

Aiello, A., Canora, F., Pasquariello, G., & Spilotro, G. (2013). Shoreline variations and coastal dynamics: A space-time data analysis of the jonian littoral, Italy. *Estuarine, Coastal and Shelf Science, 129*, 124–135.

Anders, F. J., & Byrnes, M. R. (1991). Accuracy of shoreline change rates as determined from maps and aerial photographs. *Shore and Beach, 59*, 17–26.

Anderson, M. E., & Smith, J. M. (2014). Wave attenuation by flexible, idealized salt marsh vegetation. *Coastal Engineering, 83*, 82–92.

Balay, M. A. (1961). *El Río de la Plata entre la atmósfera y el mar*. Vol. Pub. H-621. Buenos Aires, Argentina: Servicio de Hidrografía Naval.

Barbier, E. B., Acreman, M., & Knowler, D. (1997). *Economic valuation of wetlands*. Gland, Switzerland: Ramsar Convention Bureau.

Bazán, J. M., & Janiot, L. J. (1991). *Zona de máxima turbidez y su relación con otros parámetros del Río de la Plata*. Documento Técnico del Departamento de Oceanografía, Servicio Hidrografía Naval.

Bértola, G. R., Cortizo, L. C., & Isla, F. I. (2009). Dinámica litoral de la costa de Tres Arroyos y San Cayetano, Buenos Aires. *Revista de la Asociación Geológica Argentina, 64*, 657–671.

Bird, M., Chua, S., Fifield, L. K., Teh, T. S., & Lai, J. (2004). Evolution of the sungei buloh–kranji mangrove coast, Singapore. *Applied Geography, 24*, 181–198.

Brinson, M. M., & Malvárez, A. I. (2002). Temperate freshwater wetlands: Types, status, and threats. *Environmental Conservation, 29*, 115–133.

Cagnoni, M., Faggi, A. M., & Ribichich, A. (1996). La vegetación de la Reserva "El Destino" (Partido de Magdalena, Provincia de Buenos Aires). *Parodiana, 9*, 25–44.

Carol, E. S., Braga, F., Kruse, E. E., & Tosi, L. (2014). A retrospective assessment of the hydrological conditions of the Samborombon coastland (Argentina). *Ecological Engineering, 67*, 223–237.

Carretero, S., Braga, F., Kruse, E. E., & Tosi, L. (2014). Temporal analysis of the changes in the sand-dune barrier in the Buenos Aires Province, Argentina, and their relationship with the water resources. *Applied Geography, 54*, 169–181.

Cavallotto, J. L., Violante, R., & Parker, G. (2004). Sea-level fluctuations during the last 8600 years in the de la Plata river (Argentina). *Quaternary International, 114*, 155–165.

Codignotto, J. O. (2009). Incremento de la Erosión en la Costa Atlántica Argentina y el Calentamiento Global. *Geomorfología y Cambio Climático, 2*, 25–30.

Codignotto, J. O., Dragani, W. C., Martin, P. B., Campos, M. I., Alonso, G., Simionato, C. G., et al. (2011). Erosión en la bahía de Samborombón y cambios en la dirección de los vientos, provincia de Buenos Aires, Argentina. *Revista del Museo Argentino de Ciencias Naturales, 13*, 135–138.

Crowell, M., & Latherman, S. P. (1991). Historical shoreline Change: Error analysis and mapping accuracy. *Journal of Coastal Research*, 839–852.

Crowell, M., Leatherman, S. P., & Buckley, M. K. (1993). Shore-line change rate analysis: Long term versus short term data. *Shore and Beach, 61*, 13–20.

D'Onofrio, E. E., Fiore, M. M. E., & Pousa, J. L. (2008). .Changes in the regime of storm surges at Buenos Aires, Argentina. *Journal of Coastal Research, 24*, 260–265.

Feagin, R. A., Irish, J. L., Möller, I., Williams, A. M., Colón-Rivera, R. J., & Mousavi, M. E. (2011). Short communication: Engineering properties of wetland plants with application to wave attenuation. *Coastal Engineering, 58*, 251–255.

Ford, M. (2013). Shoreline changes interpreted from multi-temporal aerial photographs and high resolution satellite images: Wotje Atoll, Marshall Islands. *Remote Sensing of Environment, 135*, 130–140.

Fucks, E. E., Schnack, E. J., & Aguirre, M. L. (2010). Nuevo ordenamiento estratigráfico de las secuencias marinas del sector continental de la Bahía Samborombón, provincia de Buenos Aires. *Revista de la Asociación Geológica Argentina, 67*, 27–39.

Gedan, K. B., Kirwan, M. L., Wolanski, E., Barbier, E. B., & Silliman, B. R. (2011). The present and future role of coastal wetland vegetation in protecting shorelines: Answering recent challenges to the paradigm. *Climate Change, 106*, 7–29.

Genz, A. S., Fletcher, C. H., Dunn, R. A., Frazer, L. N., & Rooney, J. J. (2007). The predictive accuracy of shoreline change rate methods and alongshore beach variation on Maui, Hawaii. *Journal of Coastal Research, 23*, 87–105.

Isacch, J., Escapa, M., Fanjul, E., & Iribarne, O. (2010). Valoración ecológica de bienes y servicios ecosistémicos en marismas del Atlántico Sudoccidental. In *Valoración de servicios ecosistémicos: Conceptos, herramientas y aplicaciones para el ordenamiento territorial* (Vol. 23, pp. 529–552).

Isla, F. I., Cortizo, L. C., & Turno Arellano, H. (2001). Dinámica y Evolución de las Barreras Medanosas, Provincia de Buenos Aires, Argentina. *Revista Brasileira de Geomorfologia, 2*, 73–83.

Jaime, P., Menéndez, A., Uriburu Quirno, M., & Torchio, J. (2002). *Análisis del régimen hidrológico de los ríos Paraná y Uruguay. Informe* LHA, 5–216. Buenos Aires, Argentina: Instituto Nacional del Agua.

Kaiser, M. F. (2009). Environmental changes, remote sensing, and infrastructure development: The case of Egypt's East Port Said harbour. *Applied Geography, 29*, 280–288.

Kuenzer, C., van Beijma, S., Gessner, U., & Dech, S. (2014). Land surface dynamics and environmental challenges of the Niger Delta, Africa: Remote sensing-based analyses spanning three decades (1986–2013). *Applied Geography, 53*, 354–368.

Le Page, B. A. (2011). *Wetlands: A multidisciplinary perspective*. Wetlands: Springer Netherlands.

Maiti, S., & Bhattacharya, A. K. (2009). Shoreline change analysis and its application to prediction: A remote sensing and statistics based approach. *Marine Geology, 257*, 11–23.

Meyer, D. L., Townsend, E. C., & Thayer, G. W. (1997). Stabilization and erosion control value of oyster cultch for intertidal marsh. *Restororation Ecololgy, 5*, 93–99.

Michener, W. K., Blood, E. R., Bildstein, K. L., Brinson, M. M., & Gardner, L. R. (1997). Climate change, hurricanes and tropical storms, and rising sea level in coastal wetlands. *Ecological Applications, 7*, 770–801.

Mimura, N. (1999). Vulnerability of island countries in the South Pacific to sea level rise and climate change. *Climate Research, 12*, 137–143.

Moore, L. J. (2000). Shoreline mapping techniques. *Journal of Coastal Research, 16*, 111–124.

Morris, J. T., Sundareshwar, P. V., Nietch, C. T., Kjerfve, B., & Cahoon, D. R. (2000). Responses of coastal wetland storising sea level. *Ecology, 83*, 2869–2877.

Morton, R. A., Miller, T. L., & Moore, L. J. (2004). National assessment of shoreline change part 1: Historical shoreline changes and associated coastal land loss along the US Gulf of Mexico. *US Geological Survey Open File Report, 1043*, 44.

Nicholls, R. J., Wong, P. P., Burket, V. R., Codignotto, J., Hay, J. E., McLean, R. F., et al. (2007). Coastal systems and low-lying areas. In *Climate change 2007: Impacts, adaptation and vulnerability*.

NRC (National Research Council). (2007). *Mitigating shore erosion along sheltered coasts*. Washington, D.C., USA: National Academy Press.

Odum, E. P. (1978). *The value of wetlands: A hierarchical approach*. American Water Resources Association.

Perillo, G. M., Wolanski, E., Cahoon, D. R., & Brinson, M. M. (2009). *Coastal wetlands: An integrated ecosystem approach*. Amsterdam, The Netherlands: Elsevier.

Piazza, B. P., Banks, P. D., & La Peyre, M. K. (2005). The potential for created oyster shell reefs as a sustainable shoreline protection strategy in Louisiana. *Restororation Ecology, 13*, 499–506.

Pousa, J., Tosi, L., Kruse, E., Guaraglia, D., Bonardi, M., Mazzoldi, A., et al. (2007). Coastal processes and environmental hazards: The Buenos Aires (Argentina) and venetian (Italy) littorals. *Environmental Geology, 51*, 1307–1316.

Romine, B. M., Fletcher, C. H., Barbee, M. M., Anderson, T. R., & Frazer, L. N. (2013). Are beach erosion rates and sea-level rise related in Hawaii. In *Global and planetary change* (vol. 108). Elsevier B.V.

Romine, B. M., Fletcher, C. H., Frazer, L. N., Genz, A. S., Barbee, M. M., & Lim, S. C. (2009). Historical shoreline change, southeast Oahu, Hawaii; applying polynomial models to calculate shoreline change rates. *Journal of Coastal Research*, 1236–1253.

Swann, L. (2008). The use of living shorelines to mitigate the effects of storm events on dauphin island, Alabama, USA. In *American fisheries society symposium* (Vol. 64).

Thieler, E. R., & Danforth, W. W. (1994). Historical shoreline mapping (I): Improving techniques and reducing positioning errors. *Journal of Coastal Research*, 549–563.

Thieler, E. R., Himmelstoss, E. A., Zichichi, J. L., & Ergul, A. (2009). *Digital Shoreline Analysis System (DSAS) version 4.0— an ArcGIS extension for calculating shoreline change*. U.S. Geological Survey Open-File Report 1278.

Tosi, L., Kruse, E. E., Braga, F., Carol, E. S., Carretero, S. C., Pousa, J. L., et al. (2013). Hydro-morphologic settings of the Samborombón Bay (Argentina) at the end of the 21st century. *Natural Hazards and Earth System Sciences, 13*, 1–12.

Vervoorst, F. B. (1967). Las comunidades vegetales de la depresion del Salado (Provincia de Buenos Aires). In *Serie fitogeográfica 7*. Buenos Aires: INTA.

Violante, R., & Parker, G. (2004). The post-last glacial maximum transgression in the de la Plata River and adjacent inner continental shelf, Argentina. *Quaternary International, 114*, 167–181.

Zedler, J. B., & Kercher, S. (2005). Wetland resources: Status, trends, ecosystem services, and restorability. *Annual Review of Environment and Resources, 30*, 39–74.

Zhang, K., Douglas, B. C., & Leatherman, S. P. (2004). Global warming and coastal erosion. *Climate Change, 64*, 41–58.